HHS Public Access

Author manuscript

Nat Cell Biol. Author manuscript; available in PMC 2015 August 01.

Published in final edited form as:

Nat Cell Biol. 2015 February ; 17(2): 113–122. doi:10.1038/ncb3091.

Lineage specificity of primary cilia in the mouse embryo

Fiona K. Bangs, **Nadine Schrode**, **Anna-Katerina Hadjantonakis**, and **Kathryn V. Anderson***

Developmental Biology Program, Sloan Kettering Institute, Memorial Sloan Kettering Cancer Center, 1275 York Avenue, New York, NY 10065 USA

Abstract

Primary cilia are required for vertebrate cells to respond to specific intercellular signals. Here we define when and where primary cilia appear in the mouse embryo using a transgenic line that expresses ARL13B-mCherry in cilia and Centrin2-GFP in centrosomes. Primary cilia first appear on cells of the epiblast at e6.0 and are subsequently present on all derivatives of the epiblast. In contrast, extraembryonic cells of the visceral endoderm and trophectoderm lineages have centrosomes but no cilia. Stem cell lines derived from embryonic lineages recapitulate the *in vivo* pattern: epiblast stem cells are ciliated, whereas trophoblast stem cells and extraembryonic endoderm stem (XEN) cells lack cilia. Basal bodies in XEN cells are mature and can form cilia when the AURKA/HDAC6 cilia disassembly pathway is inhibited. The lineage-dependent distribution of cilia is stable throughout much of gestation, defining which cells in the placenta and yolk sac are able respond to Hedgehog ligands.

Primary cilia are microtubule-based organelles templated by centrioles that project from the surface of most vertebrate cells and are required for the responses to specific intercellular signals[1]. The regulation of cilia formation during the cell cycle has been studied in cultured cell lines, and anatomical surveys of adult tissues have shown that many cells are ciliated, but some cells, like acinar cells of the pancreas, are not ciliated, and cilia are frequently absent in tumors[2–4]. Despite the importance of cilia for mammalian biology, the rules and mechanisms that determine whether a particular cell type will have primary cilia *in vivo* are unknown.

ARL13B is a small GTPase that is strongly and specifically localized to the cilia membrane[5,6]. To study the temporal and spatial regulation of cilia formation *in vivo*, we generated a double transgenic mouse line that expressed both ARL13B fused to the monomeric red fluorescent protein mCherry[7] and Centrin2, a centriolar protein, fused to GFP[8]. Homozygous ARL13B-mCherry transgenic animals had fluorescently labeled cilia and were viable and fertile, indicating the transgene did not interfere with normal cilia function (Supplementary Figure 1A–L).

*Corresponding author k-anderson@ski.mskcc.org.

Competing financial interests

The Authors declare no competing financial interests.

Primary cilia appear after implantation only on epiblast cells

Using the ARL13B-mCherry Centrin2-GFP double transgenics, we examined the temporal and spatial pattern of centrosomes and cilia during embryonic development. Centrin2-GFP+ centrioles were readily detected in both ICM and trophectoderm cells in 32 cell blastocysts (Fig. 1A, B; Supplementary Video 1), consistent with previous observations[9,10]. In contrast, no ARL13B-mCherry expression was observed in either the ICM (0/46 cells) or trophectoderm cells (0/86 cells) of these embryos (Fig. 1A, B). Small puncta of ARL13B-mCherry were detected adjacent to the centrosomes in ~2% of ICM cells in blastocysts with 64–100 cells (Fig. 1C, D, arrow; 2 puncta/107 cells scored from 9 embryos; Supplementary Video 2), but these puncta did not display cilia morphology and did not express the cilia marker acetylated α-tubulin (Supplementary Figure 1M). No ARL13B-mCherry expression was detected in trophectoderm cells at this stage (Fig. 1C; 0/255 cells from 9 embryos).

Cilia were first detected after implantation on epiblast cells, at the time of cavitation (e5.5). At this stage, elongated ARL13B-mCherry cilia adjacent to Centrin2-GFP centrioles were detected in a small fraction (<1%) of epiblast cells (Fig. 1E, F; 3/654 epiblast cells from 10 embryos; Supplementary Video 3). By e6.0, elongated ARL13B-mCherry+ primary cilia were present on 32.7 ± 7.3% epiblast cells (Fig. 1G, H, arrows; 388/1039 epiblast cells from 6 embryos; Supplementary Video 4). At e8.0, mCherry+ primary cilia were detected on all non-dividing epiblast derived cells of the three germ layers, ectoderm, mesoderm and definitive endoderm (Fig. 1I, J; Supplementary Video 5), including cells of the embryonic node (Fig. 1K). At midgestation (e10.5), mCherry-expressing cilia projected from Centrin2-GFP+ centrioles in cells throughout the embryo, including limb mesenchyme (Fig. 1L) and neural epithelial cells (Fig. 1M).

In contrast to the presence of primary cilia on epiblast cells at e6.0, cilia were never detected on cells of extraembryonic lineages, the visceral endoderm (Fig. 1H, asterisk) and extraembryonic ectoderm (0/837 cells from 6 embryos, ~140 cells analyzed/embryo). Antibody staining confirmed that ARL13B and IFT88-positive primary cilia were present only on epiblast cells and not cells of the visceral endoderm in e6.0 embryos (Supplementary Figure 1N, O; 0/659 cells from 5 embryos, ~130 cells per embryo).

The presence of primary cilia on epiblast cells and not on cells of extraembryonic lineages was particularly striking in the e7.5 endoderm, which is composed of two intermixed populations, the embryonic visceral endoderm, which is derived from the extraembryonic lineage of the primitive endoderm and expresses alpha fetoprotein (AFP), and definitive endoderm, which is derived from cells of the epiblast that have gastrulated through the primitive streak[11,12]. At e6.5, before gastrulation has begun, AFP-GFP-expressing visceral endoderm cells form a continuous layer of cells on the outside of the embryo, but no ARL13B-mCherry labeled cilia were detected on AFP-GFP+ cells (Fig. 2A–C), although cilia were clearly present on epiblast cells (Fig. 2C, arrow). Once gastrulation began, ciliated definitive embryonic endoderm cells intercalated into the outer layer between the AFP-GFP + extraembryonic visceral endoderm cells (Fig. 2D–F). By early bud stages (e7.5) most of the endodermal layer of the embryo was composed of streak-derived definitive endoderm cells and these cells were ciliated, whereas the AFP-GFP expressing cells in the endoderm

layer still lacked ARL13B-mCherry+ primary cilia (Fig. 2G–I; Supplementary Video 6). Thus the presence of primary cilia in cells of the endoderm was determined by their cell lineage and not by their position in the embryo. At e8.0, there were still no ARL13B-mCherry+ cilia detectable on cells derived from the trophoblast lineage (ectoplacental cone and extraembryonic ectoderm; Fig. 2J–L) or the extraembryonic visceral endoderm (Fig. 2M, N).

Lineage specific assembly of primary cilia persists through gestation

The absence of cilia in the trophoblast and visceral endoderm lineages persisted later in gestation. In the labyrinth layer of the e14.5 placenta, no ARL13B+ primary cilia were detected on syncytiotrophoblast cells of the trophoblast lineage (Fig. 3A–C, arrowheads), while epiblast-derived cells that surround the fetal blood vessels were ciliated (Fig. 3D, arrows). The yolk sac includes cells derived from both the extraembryonic visceral endoderm and the epiblast-derived mesoderm. At e14.5, ARL13B-mCherry+ primary cilia were present on 57.4 ± 8.1% of mesoderm-derived mesothelial cells (Fig. 3E arrow, G arrows; 221/386 cells from 2 embryos) and 33.4 ± 3.1% of mesoderm-derived endothelial cells (Fig. 3F, G arrowheads; 95/292 cells from 2 embryos) that surrounded the blood vessels in the yolk sac, labeled with PECAM (Fig. 3G). In contrast, no ARL13B-mCherry+ cilia were seen associated with Centrin2-GFP+ centrosomes in the cells of extraembryonic visceral endoderm-derived layer of yolk sac cells (Fig. 3F, G triangles; 0/1032 cells from 2 embryos).

Stem cell lines stably recapitulate the *in vivo* pattern of ciliogenesis

Stem cell lines that stably retain the developmental potential of each of the lineages of the early mouse embryo can be derived and maintained in culture[13]; we therefore tested whether the lineage dependence of cilia formation was reflected in these stem cell lines. We derived mouse embryonic stem cells (mESCs) from double transgenic embryos under 2i+LIF conditions that promote ground state pluripotency[14] and observed that 18% of mESCs were ciliated (Fig. 4A), similar to previous results in standard mESC conditions[15]. Trophoblast stem cells (TSC) and extra-embryonic endoderm stem cells (XEN) retain the ability to differentiate into the trophoblast-derivatives of the placenta[16] and extraembryonic endoderm derivatives[17], respectively, in chimeras. TSCs, marked by expression of Eomes[18], were not ciliated, as shown by lack of acetylated α-tubulin+ structures adjacent to γ-tubulin+ centrosomes (Fig. 4B; Supplementary Figure 2A–D). In XEN cells derived from ARL13B-mCherry Centrin2-GFP transgenic embryos, no focal ARL13B-mCherry was detected adjacent to Centrin2-GFP+ centrosomes (Fig. 4C), even though Western blotting showed that ARL13B-mCherry was expressed in these cells (Supplementary Figure 2I). Antibody staining for ARL13B or acetylated α-tubulin confirmed that XEN cells, marked by expression of Sox17, did not form primary cilia (Fig. 4D, F–N, P–V; Supplementary Figure 2E–H). Epiblast stem cells (EpiSCs) represent the state of the epiblast from post-implantation embryos[19,20]. Like the cells of the e6.5 epiblast, ARL13B immunostaining showed that almost every non-mitotic cell in EpiSC colonies was ciliated (Fig. 4E; 87.2 ± 8.4%). Thus there was a correlation between the presence of cilia in the embryo and in the corresponding stem cell line: primary cilia are present on embryonic epiblast and its

derivatives and in EpiSCs, whereas cilia are not present on visceral endoderm or trophectoderm cells in the embryo or in XEN or trophoblast stem cell lines.

XEN cells are believed to be more similar to embryonic parietal endoderm than visceral endoderm[17]. We therefore added the GSK3β inhibitor CHIR99201 to convert XEN cells into visceral endoderm[21]. This treatment caused upregulation of FoxA2, a visceral endoderm specific transcription factor (Supplementary Figure 2J), and caused a transition from a rounded XEN cell morphology to an epithelial morphology and upregulation of E-Cadherin, as in the visceral endoderm (Supplementary Figure 2L). Antibody staining for acetylated α-tubulin and γ-tubulin showed that these cells lacked primary cilia (Supplementary Figure 2K, M), demonstrating that visceral endoderm cells derived from XEN cells lack primary cilia, like visceral endoderm cells in the embryo.

Removal of serum from many cultured cells triggers exit from the cell cycle and promotes cilia formation[2]. In contrast, withdrawal of serum from XEN cells did not lead to cilia assembly (Fig. 4D; 0/267 cells from 2 independent experiments) and the EpiSCs that formed cilia were grown in the presence of serum. Thus mechanisms that have been described in cell culture may not regulate cilia formation in embryo-derived stem cell lines.

XEN cell basal bodies are mature but do not nucleate cilia

The absence of cilia in XEN cell lines made it possible to test why cilia fail to form in this lineage. Transcription factors of the RFX family promote the expression of genes required for ciliogenesis[22] and RFX3 is required for the formation of normal primary cilia in the mouse embryo[23]. RFX3 was highly expressed in epiblast cells and at lower levels in visceral endoderm cells (Supplementary Figure 3A, B) however RFX3 was expressed in all nuclei in both mESCs (Supplementary Figure 3C, D) and XEN cells (Supplementary Figure 3E, F), indicating the RFX3 is not the factor that determines which lineages are ciliated.

For ciliogenesis to initiate, the mother centriole must mature into a basal body with distal appendages that dock the mother centriole to the plasma membrane and sub-distal appendages that mediate attachment to microtubules; after membrane attachment, proteins of the ciliary transition zone are recruited[24]. CEP164, a centrosomal distal appendage protein, and Ninein, a subdistal appendage protein, were both localized to the distal end of mother centrosomes in XEN cells (Fig. 4F, H), as in ciliated mouse embryonic fibroblasts (MEFs) and EpiSCs (Fig. 4G, I; Supplementary Figure 3G, H). In cycling fibroblasts, serum withdrawal triggers the recruitment of positive regulators to the distal tip of the mother centriole, including the kinase TTBK2, which acts at the mother centriole to recruit intraflagellar transport (IFT) proteins and initiate axoneme assembly[25]. Antibody staining showed that TTBK2 and IFT88 both localized to the distal end of the mother centriole in XEN cells (Fig. 4J, L), as in ciliated MEFs and EpiSCs, where IFT88 was also present in the axoneme (Fig. 4K, M; Supplementary Figure 3I, J). In addition, the transition zone proteins NPHP4, MKS1, CEP290 and Inversin were present at centrioles in XEN cells (Fig. 4N, P, R, T), as in ciliated MEFs (Fig. 4O, Q, S, U). Thus the basal bodies in XEN cells appear to be poised to make cilia.

The initiation of ciliogenesis is associated with removal of negative regulators, including CP110, from the distal tip of the mother centriole[26,27]. In ciliated MEFs and EpiSCs CP110 was only present on the daughter centriole and was absent from the mother centriole (Fig. 4W; Supplementary Figure 3K), while CP110 localized to both the mother and daughter centrioles in XEN cells (Fig. 4V) and in cells of the embryonic visceral endoderm at e6.5 (Fig. 4X, arrows). We used siRNA to partially (68%) knockdown expression of CP110. In those knockdown cells where CP110 could not be detected at the centriole, cilia were not formed, as no ARL13B+ or IFT88+ axonemes were detected (Supplementary Figure 3P, R). Instead, as in U2OS osteosarcoma cells[27,28], knockdown of CP110 in XEN cells caused formation of elongated centrioles (16.6 ± 7.7%, 65/503 cells), distinguished by expression of γ–tubulin and Centrin2-GFP along their length (Supplementary Figure 3L–R) and IFT88 at the distal end of the mother centriole (Supplementary Figure 3P). Thus the presence of CP110 on centrioles does not account for the lack of cilia in XEN cells.

Recently, a number of proteins and factors, including Plk1, APC/C and ceramide, have been reported to regulate ciliogenesis in specific cell types[29–31]. We did not detect any role for these components in regulation of cilia formation in XEN cells (Supplementary Figure 4).

The cilia disassembly pathway is active in XEN cells

When a cell enters mitosis, the primary cilium is disassembled and the mother centriole is recruited to one of the poles of the mitotic spindle. The mitotic regulatory kinase Aurora kinase A (AURKA) plays an important role in cilia disassembly at mitosis[32]; we therefore tested whether elevated activity of AURKA could be responsible for the absence of cilia in XEN cells. The total level of AURKA in XEN cells was 1.8 times that in EpiSCs (Fig. 5A, B) and the ratio of activated AURKA to total AURKA was 2.4-fold higher in XEN cells than in EpiSCs (Fig. 5B); thus there was 4.3-fold more activated AURKA in (unciliated) XEN cells than in (ciliated) EpiSCs. Activation of AURKA depends on its association with the scaffolding protein NEDD9 (formerly HEF1)[32]. Western blot and qPCR analyses showed that NEDD9 protein levels were 2.6 ± 1.2 times higher in XEN cells than in EpiSCs (Fig. 5C, D) and *Nedd9* mRNA levels were ~3.6 times higher (Fig. 5E), consistent with higher levels of active AURKA.

Blocking the cilium disassembly pathway permits cilia assembly in extraembryonic cells

To test whether lack of primary cilia on XEN cells was caused by increased AURKA activity, we cultured XEN cells in the presence of the AURKA inhibitor Alisertib (MLN8237)[33]. Treatment with 250 nM Alisertib for 16 h reduced levels of phosphorylated AURKA by 32.5 fold (Fig. 6A) and active AURKA could no longer be detected at the spindle pole (Supplementary Figure 5A–F). After drug treatment, 6.6 ± 2.7% of XEN cells were ciliated (20/328 cells, n=328 cells pooled from 2 independent experiments), compared to 0% in DMSO treated control cells (0/392 cells, n=392 cells pooled from 2 independent experiments; $p<0.0001$ from t-test). Removal of serum did not increase the number of cilia assembled (6.03 ± 1.5% cilia; 15/256 cells, n=256 cells pooled from 2 independent experiments, DMSO control 0/215 cells, n=215 cells pooled from 2 independent

experiments; p<0.0001 from t-test). Treatment with 5 μM PHA680632, a second, albeit less specific, AURKA inhibitor, induced formation of primary cilia on 5.1 ± 1.7% of XEN cells (15/302 cells, n=302 cells pooled from 3 independent experiments) after 72 h, compared to 0% in DMSO treated control cells (0/533 cells, n=533 cells pooled from 3 independent experiments; p<0.0001 from t-test). Higher doses of the inhibitors caused profound defects in mitosis and a high rate of cell death, as expected, although up to 17% of the surviving cells were ciliated (17.2 ± 0.2% 15/87 cells, n=87 cells pooled from 2 independent experiments) following treatment with 10μM PHA680632 for 72 hours (DMSO control 0/447 cells, n=447 cells pooled from 2 independent experiments; p<0.0001 from t-test). The primary cilia that formed in the presence of the inhibitors appeared to be structurally normal, with axonemes that contained acetylated microtubules and IFT88, as well as an ARL13B+ ciliary membrane (Fig. 6C–F). After treatment, XEN cells still expressed Sox17, indicating that AURKA inhibition had not changes the identity of the cells (Supplementary Figure 5G, H).

To confirm these findings, we knocked down AURKA in XEN cells. siRNA treatment reduced total AURKA to 15% the level present in untreated cells (Fig. 6B;), although AURKA could still be detected at the centrosome (Supplementary Figure 5I–N). After knockdown, 1.2 ± 1.1% of XEN cells were ciliated (Fig. 6G; 7/610 cells, n=610 cells pooled from 2 independent experiments) compared to 0% of cells (0/600 cells, n=600 cells pooled from 2 independent experiments, p=0.0185 from t-test) treated with a scrambled control siRNA.

AURKA promotes cilia disassembly, at least in part, by activation of the tubulin deacetylase HDAC6, which deacetylates ciliary microtubules and leads to collapse of the cilium[32]. Tubacin, a specific inhibitor of HDAC6, blocks serum-induced cilia disassembly[34]. After 12 h of 5 μM tubacin treatment, cilia were detected on 1.1 ± 1.0% XEN cells (Fig. 6H, I; 8/717 cells) but this was not significantly different from DMSO controls (0/516 cells from 3 independent experiments). After 72 h of 5 μM tubacin treatment, 3.9 ± 2.3% of XEN cells (22/573 cells, n=573 cells pooled from 3 independent experiments) formed a cilium (Supplementary Figure 5O, P), significantly different from 0% in DMSO controls (0/433 cells, n=433 cells pooled from 3 independent experiments; p<0.0001 from t-test). To test whether the AURKA-HDAC6 pathway regulates cilia formation in the visceral endoderm *in vivo*, we cultured embryos that expressed both AFP-GFP, to mark the visceral endoderm[11], and ARL13B-mCherry, to mark cilia, in 5 μM tubacin for 12 h. This treatment effectively increased cytoplasmic microtubule acetylation (Supplementary Figure 5Q–T; pixel intensity DMSO =1, tubacin =4.6). In tubacin-treated embryos 2.6 ± 1.9% of visceral endoderm cells were ciliated (Fig. 6K, arrow, 30/1313 cells, n=1313 cells counted across 7 embryos), which was significantly different from 0% in DMSO controls (Supplementary Fig. 6J; 0/1263 cells, n=1263 cells counted across 6 embryos; p=0.0065 from t-test). These experiments demonstrate that mother centrioles in XEN and VE cells can template cilia in extraembryonic lineages *in vivo* when the cilium disassembly pathway is blocked.

In cystic renal disease, loss of VHL leads to loss of cilia through activation of AURKA and NEDD9[35], when GSK3β is inactive[36]. Western blot analysis showed that VHL protein was present at equivalent levels in XEN cells and EpiSCs (Supplementary Figure 4A, n=3 from 2

independent experiments). Thus VHL protein is not limiting for cilia formation in XEN cells. VHL regulates the stability of the α-subunit of hypoxia inducible factor (HIF) 1α and HIF2α which in turn can active NEDD9 and AURKA[35]. 24h treatment of XEN cells with 1μM FM19G11, which blocks the function of both HIF1α and HIF2α (IC50 = 80nM[37]) does not cause cilia formation (4B, C; 0/284 cells; DMSO 0/278 cells; from 2 independent experiments). Thus, in XEN cells, NEDD9 and AURKA are activated by a HIF-independent pathway to inhibit cilia formation.

Discussion

Our studies show that cilia formation in vivo is controlled by stable lineage-based mechanisms. In contrast to studies in cell culture, which have focused on the formation of cilia in response to serum withdrawal, we find that stem cell lines make stem cells based on their lineage: visceral endoderm and XEN cells fail to form cilia while embryonic epiblast and epiSCs grow cilia, independent of the presence of serum. The basal bodies in XEN cells are mature; they contain all the tested components of the ciliary appendages and transition zone, as well as IFT88 and the cilia-initiating kinase TTBK2, but fail to grow a ciliary axoneme. The maturity of these basal bodies is demonstrated by the formation of cilia when the AURKA/HDAC6 cilia disassembly pathway is blocked. As only a relatively small fraction of XEN cells are ciliated after inhibition of AURKA/HDAC6, there could be an additional, previously undescribed pathway that blocks cilia formation in XEN and visceral endoderm cells. Alternatively, it is possible that activation of the cilia disassembly pathway is sufficient to account for the absence of cilia in XEN cells, but the essential role of AURKA in mitosis prevents a straightforward test of that hypothesis. Nevertheless, the identification of stem cell lines that differentially regulate ciliogenesis provides a foundation for further dissection of the regulatory networks that control cell-type specific cilia formation in vivo.

The lineage dependence of cilia in the mouse embryo implies that cells of extraembryonic origin cannot respond to specific developmental signals; in particular, these cells must be unable to respond to Hedgehog (Hh) ligands[1]. The first time that Hh signaling is known to be active in the mouse embryo is at the beginning of gastrulation, when Indian Hedgehog (Ihh) expressed in the extraembryonic visceral endoderm signals to the adjacent extraembryonic mesoderm to promote blood island formation[38,39]. Ihh is also expressed at later stages in yolk sac, and the only cells in the placenta that express the Hh target gene *Patched1* are in the embryo-derived cells that surround the fetal blood vessels[40]. Not only do XEN cells lack cilia, they also do not express essential components of the Hh signal transduction pathway, including Ptch1, Smo and Gli transcription factors[20,38,41]; thus it appears that visceral endoderm cells are programmed in several ways to prevent responses to the Hh ligands that they produce. The data suggest that normal development of the placenta and yolk sac depends on preventing Hh target gene expression in extraembryonic lineages.

Methods

Mouse strains

The species used in this study was *Mus musculus*. To generate ARL13B-mCherry transgenics, the coding region of an *Arl13b* cDNA was fused in-frame upstream of mCherry then inserted into pCAGGs, which contains a chicken β–actin promoter and CMV immediate early enhancer[42]. The resulting pCAG-ARL13b:mCherry construct was linearized, purified and introduced into FVB oocytes via pro-nuclear injection by the MSKCC Mouse Genetics Core Facility. Four founder lines were identified; transgene expression was only consistent in one line. This single line was used for all experiments.

ARL13B-mCherry; Centrin-GFP and ARL13B-mCherry;AFP-GFP were both on a mixed background of FVB and C3H. Other mouse strains used were *Arl13b*$^{hnn\ 5}$, Centrin2-GFP[8], and AFP-GFP[11]. Embryos ranging from embryonic day 3.5 to 14.5 as well as adult males and females for breeding between 8 weeks to 6 months and females for embryos between 8–10 weeks were used for this study. Animals were housed and bred under standard IACUC guidelines. The MSKCC IACUC approved these experiments.

ESC and XEN cell derivation and differentiation

mESCs were derived as described previously[43], maintained on Mitomycin-C treated feeder cells and grown in KnockOut DME (Gibco) supplemented with 15% fetal bovine serum (HyClone), 2mM L-Glutamine (Gibco), 0.1mM β-mercaptoethanol (Gibco), 0.1mM Non essential amino acids (Gibco), 1mM Sodium Pyruvate (Gibco), 1% v/v penicillin and streptomycin (Gibco), 1000 units LIF (millipore), 1μM PD0325901 and 3μM SHIR99021 (Stemgent). XEN cells were derived as described previously[44], maintained on 1% gelatin coated plastic dishes and grown in RPMI1640 (pH 7.2) (Gibco) supplemented with 15% fetal bovine serum (HyClone), 2mM L-Glutamine (Gibco), 0.1mM β-mercaptoethanol (Gibco), 0.1mM Non essential amino acids (Gibco), 1mM Sodium Pyruvate (Gibco) and 1% v/v penicillin and streptomycin (Gibco).

XEN cells were differentiated into visceral endoderm via addition of 3μM CHIR99021 (Stemgent) for 3 days[21]. EpiSCs were provided by M. Tomishima and cultured as per[45].

TSCs were provided by A–K. Hadjantonakis and grown in RPMI1640 (pH 7.2) supplemented with 20% FBS, 100 μM β-mercaptoethanol, 2 mM L-glutamine, 1 mM sodium pyruvate, 1% v/v penicillin and streptomycin (Gibco), 25 ng/mL FGF4 (PeproTech) and 1 μg/mL Heparin (Sigma-Aldrich). Newly derived mESC and XEN cell lines tested negative for mycroplasma.

Primary MEF cells were derived from e10.5 wild type embryos by gentle pipetting in 0.5% trypsin/EDTA (Gibco). MEF cells were grown in DME supplemented with 15% bovine calf serum (BenchMark), 2 mM L-glutamine, 1% v/v penicillin and streptomycin (Gibco). To induce cilia, confluent MEFs were serum starved for 24 h. Cells lines were not authenticated by STR profiling. Newly derived mESC and XEN cell lines tested negative for mycroplasma.

Drug treatments

XEN cells were split 1:10 then treated for the indicated time period either immediately in 5 and 10 μM PHA680632 (Sellechem), 5 μM Tubacin (Chemie Tek), or 24 h after splitting in 250nM Alisertib (Sellechem), 1 μM FM19G11 (Sigma), 1 μM BI2536 (Sellechem), 2 and 20 μM N-nervonoyl d-erythro sphingosine (C24:1) ceramide (Avanti polar Lipids), 20 μM proTAME (R&D Systems). All inhibitors were diluted in DMSO apart from N-nervonoyl d-erythro sphingosine (C24:1) ceramide, which was diluted in chloroform.

siRNA knock down

XEN cells were split 1:10 and immediately transfected with siRNAs using Lipofectamine RNAiMAX (Invitrogen). AurkA knock down was performed using a pool of 4 GeneSolution siRNAs (1027416, Qiagen) Mm_AurkA_1_CACCTGTGTCGTAGCCTTCAA, Mm_AurkA_2_CAGAGTGTGTGTATAACTTAT, Mm_AurkA_3_CTCTGTCTTACTGTCATTCAA, Mm_AurkA_4_ACCCGAGTTTATCTGATTCTA at 90pMol each. CP110 knock down was performed using siGENOME SMARTpool (ThermoScientific) at 90pMol.

Embryo Culture

Embryos for culture were dissected in M2 culture media (Millipore) keeping the ectoplacental cone intact, removing Reichart's membrane, then transferred to a glass-bottomed culture dish in 50% rat serum/50% DMEM/F12 and incubated at 37°C with 5% CO2 for 12 h in 5μM Tubacin diluted in DMSO.

Immunofluorescence staining

Cells were seeded onto fibronectin (Millipore) coated glass coverslips (Warner Instruments). Fixed in 4% P.F.A at room temperature 5 min, then 100% Methanol at −20°C 5 min. Blocked in 0.3% Triton-X100+3%BSA+5%serum in PBS.

Blastocysts were stained in U bottomed 96 well plates coated with 1% Agar / 0.9% NaCl and transferred between wells with a pulled glass pipette. Blastocysts were fixed in 4% paraformaldehyde (PFA) for 5 mins, washed 3 times in 0.1% Triton X-100 / PBS, the zona pellucida was removed with Acid Tyrodrodes solution for 1 min, permeabilized in 0.5% Triton X-100 / 100mM Glycine / PBS for 5 mins, washed, blocked in 2% Goat serum / PBS for 1 h, primary antibody was diluted in blocking solution and incubated at 4°C over night. Blastocysts were then washed 3 times in 0.1% Triton X-100 / PBS, incubated with secondary antibody for 1 h, washed and imaged in 0.1% Triton X-100 / PBS on a glass bottomed MatTek dish.

Post implantation embryos were fixed for 1 h at room temperature in 4% PFA, washed in 0.1% Triton X-100 / PBS. Embryos were blocked over night in 0.1% Triton-X100 / 5% goat serum / PBS at 4°C on a rocking platform. Primary antibody was diluted in blocking buffer and incubated overnight at 4°C. Embryos were washed 5 times for 2 h in 0.1% Triton X-100 / PBS, then over night. Secondary antibody was diluted in blocking buffer and incubated for 2 h at 4°C. Embryos were washed a further 5 times for 2 h in 0.1% Triton

X-100 / PBS, then over night before mounting in 2% low melting point agarose on glass bottomed MatTek dishes and sealed with Vectasheild mounting media (Vectorlabs).

For neural tube, placenta and yolk sac embryos were fixed in 2% PFA at 4°C over night, embedded in OCT and cryosctioned at 12μm. Slides were mounted in Vectashield (Vectorlabs). For immunofluorescence staining yolk sac sections were boiled for 10 mins in 10mM NaCitrate. All sections were washed with PBS, blocked in 1% goat serum / PBS for 30 mins. Primary antibody was diluted in blocking buffer and incubated 4°C over night. Sections were washed 4 times in blocking buffer, incubated in secondary antibody for 1 h at room temperature. Slides were mounted with Prolong Gold mounting media (LifeTechnologies).

Antibodies used were: FOXA2 (1:1000 Ab40874), ISLET1 and PAX7 (1:10 DSHB), NKX2.2 (1:2 DSHB), SMO (1:500;[46]), GLI2 (1:1000, gift J Eggenschwiler[47]), ARL13B (1:500, gift T. Caspary[5]), NANOG (1:500, eBiosciences 14-5761-80), SOX17 (1:500, R&D AF1924), EOMES (1:500, Abcam 23345), HNF4α (1:500, Santa Cruz C-19), CP110 (1:500, ProteinTech 12780-1-AP), CEP164 (1:500, Sdix 4533.00.02), NINEIN (1:1000, gift J Sillibourn and M Bornens[48]), TTBK2 (1:500, Sigma Prestige HPA018113), IFT88 (1:500, ProteinTech 13967-1-AP), RFX3 (1:200, Sigma Prestige HPA035689), E-Cadherin (1:200, Sigma U3254), Acetylated α-tubulin (1:1000, Sigma T6793), γ–tubulin (1:1000, Sigma T6557), MKS1 (1:20, ProteinTech 16206-1-AP), NPHP4 (1:20, ProteinTech 13812-1-AP), CEP290, (1:100, Novus Biologicals NB100-86991), Inversin (1:10, T. Yokoyama[49]), PECAM (1:200, BD Pharmingen 550274).

Western blot analysis

Cells were lysed in standard RIPA buffer (0.15 mM NaCl/0.05 mM Tris-HCl, pH 7.2/1% Triton X-100/1% sodium deoxycholate/ 0.1% SDS) with phosphatase inhibitor cocktails 1 and 2 (Calbiochem) at 4°C for 30 min and centrifuged at 13,000rpm for 10 min. Lysates were run on 8–12% polyacrylamide gels transferred onto PVDF either for 1 h at room temperature at 100V (pVHL) or at 4°C over night at 30V. Membranes were blocked in 5%BSA or 5% Non-fat Milk in TBST. Antibodies; AurkA (1:1000, BD biosciences 610938 IAK1), pAurkA (T288) (1:100, Cell Signaling C39D8), Hef1 (1:1000, Abcam 166663), mCherry (1:1000 Clontech), VHL (1:1000, Cell signaling 2738), GAPDH (1:1,000, Santa Cruz 25778).

Imaging

Wholemount embryos were imaged on a Leica TCS SP8 inverted laser scanning confocal microscope and deconvolved using AutoQuantX3. Cells were imaged using an inverted Deltavision Image Restoration Microscope. Sections and images for quantification were imaged on an upright Zeiss Axio2Imaging microscope.

Reproducibility of Experiments and Statistical Tests

Sample sizes were determined by the nature of the experiment and variability of the output not via a statistical method. Numbers of embryos and cells measured are indicated in the text and figure legends. For observations in embryos 3–10 ARL13B-mCherry; Centrin2-GFP

embryos were analyzed at each stage. Between 3 and 4 ARL13B-mCherry; AFP-GFP embryos were analyzed at each stage. Given consistency of results this was considered sufficient. For cilia numbers in embryos 46-1039 cells were counted from 2–6 embryos. Cilia length was calculated from 3 wild type and 3 transgenic embryos. For cell based assays 6–23 fields of cells with a total of at least 200 cells were counted from 2 or 3 independent biological replicates. Drug treatments that did not result in assembly of primary cilia were only performed once. Western blots and qPCR were repeated 2–3 times as indicated in the text and figure legends. All correctly processed and imaged samples were included. Figure 1A, B show representative data from 4 embryos, C, D from 9 embryos, E, F from 10 embryos, G, H from 6 embryos, I-K 2 from embryos. Figure 2 A–C show representative data from 4 embryos, D-I from 3 embryos. Figure 3E–G show representative data from 2 embryos. Figure 4 A–C show representative data from 3 independent experiments, D from 2 independent experiments, D from 3 independent experiments, F-W from 3 independent experiments and X from 2 independent experiments. Figure 5 shows representative data from 3 independent experiments. Figure 6A–D shows representative data from 2 independent experiments E, F from 3 independent experiments, G from 2 independent experiments, H, I from 3 independent experiments, J from 6 independent experiments and K from 7 independent experiments. Supplementary Figure 1A–F show representative data from 2 independent experiments, H-L from 10 independent experiments, M from 9 independent experiments, N, O from 5 independent experiments. Supplementary Figure 2A–H show representative data from 3 independent experiments, I from 1 independent experiment and J-M from 2 independent experiments. Supplementary Figure 3A–F and G-K show representative data from 2 independent experiments and L-S from 3 independent experiments. Supplementary Figure 4A–C show representative data form 2 independent experiments. Supplementary Figure 5A–H shows representative data from 2 independent experiments, I-N from 2 independent experiments, O, P from 3 independent experiments, Q-T from 2 independent experiments. The experiments were not randomized and the investigators were not blinded to allocation during experiments or when assessing the outcome of experiments. Mean averages are given ± standard deviation. Students t-test was used for statistical analysis.

Supplementary Material

Refer to Web version on PubMed Central for supplementary material.

Acknowledgements

We thank Hisham Bazzi and Sarah Goetz for comments on the manuscript and Meg Distinti for help with manuscript preparation. We thank the MSKCC Mouse Genetics Facility for help making the transgenic mice, and the Molecular Cytology Facility and the Rockefeller University Bio-Imaging Resource Center for help with imaging. This work was supported by National Institutes of Health grants NS044385 and HD035455 to K. V. Anderson, a NYSTEM postdoctoral fellowship to F. Bangs, NYSTEM grant 029568 to A.-K. Hadjantonakis and the MSKCC Cancer Center Support Grant (P30 CA008748).

References

1. Goetz SC, Anderson KV. The primary cilium: a signalling centre during vertebrate development. Nat Rev Genet. 2010; 11:331–344. [PubMed: 20395968]

2. Seeley ES, Nachury MV. The perennial organelle: assembly and disassembly of the primary cilium. J. Cell. Sci. 2010; 123:511–518. [PubMed: 20144999]
3. Wong SY, et al. Primary cilia can both mediate and suppress Hedgehog pathway–dependent tumorigenesis. Nat Med. 2009; 15:1055–1061. [PubMed: 19701205]
4. Han Y-G, et al. Dual and opposing roles of primary cilia in medulloblastoma development. Nat Med. 2009; 15:1062–1065. [PubMed: 19701203]
5. Caspary T, Larkins CE, Anderson KV. The Graded Response to Sonic Hedgehog Depends on Cilia Architecture. Developmental Cell. 2007; 12:767–778. [PubMed: 17488627]
6. Larkins CE, Aviles GDG, East MP, Kahn RA, Caspary T. Arl13b regulates ciliogenesis and the dynamic localization of Shh signaling proteins. Molecular Biology of the Cell. 2011; 22:4694–4703. [PubMed: 21976698]
7. Shaner NC, et al. Improved monomeric red, orange and yellow fluorescent proteins derived from Discosoma sp. red fluorescent protein. Nature biotechnology. 2004; 22:1567–1572.
8. Higginbotham H, Bielas S, Tanaka T, Gleeson JG. Transgenic mouse line with green-fluorescent protein-labeled Centrin 2 allows visualization of the centrosome in living cells. Transgenic Res. 2004; 13:155–164. [PubMed: 15198203]
9. Courtois A, Schuh M, Ellenberg J, Hiiragi T. The transition from meiotic to mitotic spindle assembly is gradual during early mammalian development. J. Cell Biol. 2012; 198:357–370. [PubMed: 22851319]
10. Gueth-Hallonet C, et al. gamma-Tubulin is present in acentriolar MTOCs during early mouse development. J. Cell. Sci. 1993; 105(Pt 1):157–166. [PubMed: 8360270]
11. Kwon GS, et al. Tg(Afp-GFP) expression marks primitive and definitive endoderm lineages during mouse development. Dev. Dyn. 2006; 235:2549–2558. [PubMed: 16708394]
12. Kwon GS, Viotti M, Hadjantonakis A-K. The Endoderm of the Mouse Embryo Arises by Dynamic Widespread Intercalation of Embryonic and Extraembryonic Lineages. Developmental Cell. 2008; 15:509–520. [PubMed: 18854136]
13. Ralston A, Rossant J. Genetic regulation of stem cell origins in the mouse embryo. Clin. Genet. 2005; 68:106–112. [PubMed: 15996204]
14. Ying Q-L, et al. The ground state of embryonic stem cell self-renewal. Nature. 2008; 453:519–523. [PubMed: 18497825]
15. Hunkapiller J, Singla V, Seol A, Reiter JF. The Ciliogenic Protein Oral-Facial-Digital 1 Regulates the Neuronal Differentiation of Embryonic Stem Cells. Stem Cells and Development. 2011; 20:831–841. [PubMed: 20873986]
16. Tanaka S. Promotion of Trophoblast Stem Cell Proliferation by FGF4. Science. 1998; 282:2072–2075. [PubMed: 9851926]
17. Kunath T. Imprinted X-inactivation in extra-embryonic endoderm cell lines from mouse blastocysts. Development. 2005; 132:1649–1661. [PubMed: 15753215]
18. Nowotschin S, et al. The T-box transcription factor Eomesodermin is essential for AVE induction in the mouse embryo. Genes Dev. 2013; 27:997–1002. [PubMed: 23651855]
19. Brons IGM, et al. Derivation of pluripotent epiblast stem cells from mammalian embryos. Nature. 2007; 448:191–195. [PubMed: 17597762]
20. Tesar PJ, et al. New cell lines from mouse epiblast share defining features with human embryonic stem cells. Nature. 2007; 448:196–199. [PubMed: 17597760]
21. Chuykin I, Schulz H, Guan K, Bader M. Activation of the PTHRP/adenylate cyclase pathway promotes differentiation of rat XEN cells into parietal endoderm, whereas Wnt/β-catenin signaling promotes differentiation into visceral endoderm. J. Cell. Sci. 2013; 126:128–138. [PubMed: 23038778]
22. Reith W, et al. RFX1, a transactivator of hepatitis B virus enhancer I, belongs to a novel family of homodimeric and heterodimeric DNA-binding proteins. Mol. Cell. Biol. 1994; 14:1230–1244. [PubMed: 8289803]
23. Bonnafe E, et al. The transcription factor RFX3 directs nodal cilium development and left-right asymmetry specification. Mol. Cell. Biol. 2004; 24:4417–4427. [PubMed: 15121860]

24. Reiter JF, Blacque OE, Leroux MR. The base of the cilium: roles for transition fibres and the transition zone in ciliary formation, maintenance and compartmentalization. EMBO reports. 2012; 13:608–618. [PubMed: 22653444]
25. Goetz SC, Liem KF Jr, Anderson KV. The Spinocerebellar Ataxia-Associated Gene Tau Tubulin Kinase 2 Controls the Initiation of Ciliogenesis. Cell. 2012; 151:847–858. [PubMed: 23141541]
26. Kobayashi T, Tsang WY, Li J, Lane W, Dynlacht BD. Centriolar Kinesin Kif24 Interacts with CP110 to Remodel Microtubules and Regulate Ciliogenesis. Cell. 2011; 145:914–925. [PubMed: 21620453]
27. Spektor A, Tsang WY, Khoo D, Dynlacht BD. Cep97 and CP110 Suppress a Cilia Assembly Program. Cell. 2007; 130:678–690. [PubMed: 17719545]
28. Schmidt TI, et al. Control of Centriole Length by CPAP and CP110. Current Biology. 2009; 19:1005–1011. [PubMed: 19481458]
29. Wang G, et al. PCM1 recruits Plk1 to the pericentriolar matrix to promote primary cilia disassembly before mitotic entry. J. Cell. Sci. 2013; 126:1355–1365. [PubMed: 23345402]
30. He Q, et al. Primary cilia in stem cells and neural progenitors are regulated by neutral sphingomyelinase 2 and ceramide. Molecular Biology of the Cell. 2014; 25:1715–1729. [PubMed: 24694597]
31. Wang W, Wu T, Kirschner MW, Nelson WJ. The master cell cycle regulator APC-Cdc20 regulates ciliary length and disassembly of the primary cilium. eLife. 2014; 3:e03083. [PubMed: 25139956]
32. Pugacheva EN, Jablonski SA, Hartman TR, Henske EP, Golemis EA. HEF1-Dependent Aurora A Activation Induces Disassembly of the Primary Cilium. Cell. 2007; 129:1351–1363. [PubMed: 17604723]
33. Nikonova AS, Astsaturov I, Serebriiskii IG, Dunbrack RL, Golemis EA. Aurora A kinase (AURKA) in normal and pathological cell division. Cell. Mol. Life Sci. 2012; 70:661–687. [PubMed: 22864622]
34. Haggarty SJ, Koeller KM, Wong JC, Grozinger CM, Schreiber SL. Domain-selective small-molecule inhibitor of histone deacetylase 6 (HDAC6)-mediated tubulin deacetylation. Proceedings of the National Academy of Sciences. 2003; 100:4389–4394.
35. Thoma CR, et al. pVHL and GSK3β are components of a primary cilium-maintenance signalling network. Nat Cell Biol. 2007; 9:588–595. [PubMed: 17450132]
36. Xu J, et al. VHL Inactivation Induces HEF1 and Aurora Kinase A. Journal of the American Society of Nephrology. 2010; 21:2041–2046. [PubMed: 20864688]
37. Moreno-Manzano V, et al. FM19G11, a New Hypoxia-inducible Factor (HIF) Modulator, Affects Stem Cell Differentiation Status. Journal of Biological Chemistry. 2010; 285:1333–1342. [PubMed: 19897487]
38. Dyer MA, Farrington SM, Mohn D, Munday JR, Baron MH. Indian hedgehog activates hematopoiesis and vasculogenesis and can respecify prospective neurectodermal cell fate in the mouse embryo. Development. 2001; 128:1717–1730. [PubMed: 11311154]
39. Farrington SM, Belaoussoff M, Baron MH. Winged-Helix, Hedgehog and Bmp genes are differentially expressed in distinct cell layers of the murine yolk sac. Mech. Dev. 1997; 62:197–211. [PubMed: 9152011]
40. Jiang F, Herman GE. Analysis of Nsdhl-deficient embryos reveals a role for Hedgehog signaling in early placental development. Hum. Mol. Genet. 2006; 15:3293–3305. [PubMed: 17028112]
41. Artus J, et al. BMP4 signaling directs primitive endoderm-derived XEN cells to an extraembryonic visceral endoderm identity. Dev. Biol. 2012; 361:245–262. [PubMed: 22051107]
42. Hitoshi N, Ken-ichi Y, Jun-ichi M. Efficient selection for high-expression transfectants with a novel eukaryotic vector. Gene. 1991; 108:193–199. [PubMed: 1660837]
43. Czechanski A, et al. Derivation and characterization of mouse embryonic stem cells from permissive and nonpermissive strains. Nat Protoc. 2014; 9:559–574. [PubMed: 24504480]
44. Niakan KK, Schrode N, Cho LTY, Hadjantonakis A-K. Derivation of extraembryonic endoderm stem (XEN) cells from mouse embryos and embryonic stem cells. Nat Protoc. 2013; 8:1028–1041. [PubMed: 23640167]
45. Chenoweth, JG.; Tesar, PJ. Methods in Molecular Biology. link.springer.com. Vol. 636. Humana Press; 2010. p. 25-44.

46. Ocbina PJR, Anderson KV. Intraflagellar transport, cilia, and mammalian Hedgehog signaling: analysis in mouse embryonic fibroblasts. Dev. Dyn. 2008; 237:2030–2038. [PubMed: 18488998]

47. Qin J, Lin Y, Norman RX, Ko HW, Eggenschwiler JT. Intraflagellar transport protein 122 antagonizes Sonic Hedgehog signaling and controls ciliary localization of pathway components. Proceedings of the National Academy of Sciences. 2011; 108:1456–1461.

48. Delgehyr N, Sillibourne J, Bornens M. Microtubule nucleation and anchoring at the centrosome are independent processes linked by ninein function. J. Cell. Sci. 2005; 118:1565–1575. [PubMed: 15784680]

49. Shiba D, et al. Localization of Inv in a distinctive intraciliary compartment requires the C-terminal ninein-homolog-containing region. J. Cell. Sci. 2009; 122:44–54. [PubMed: 19050042]

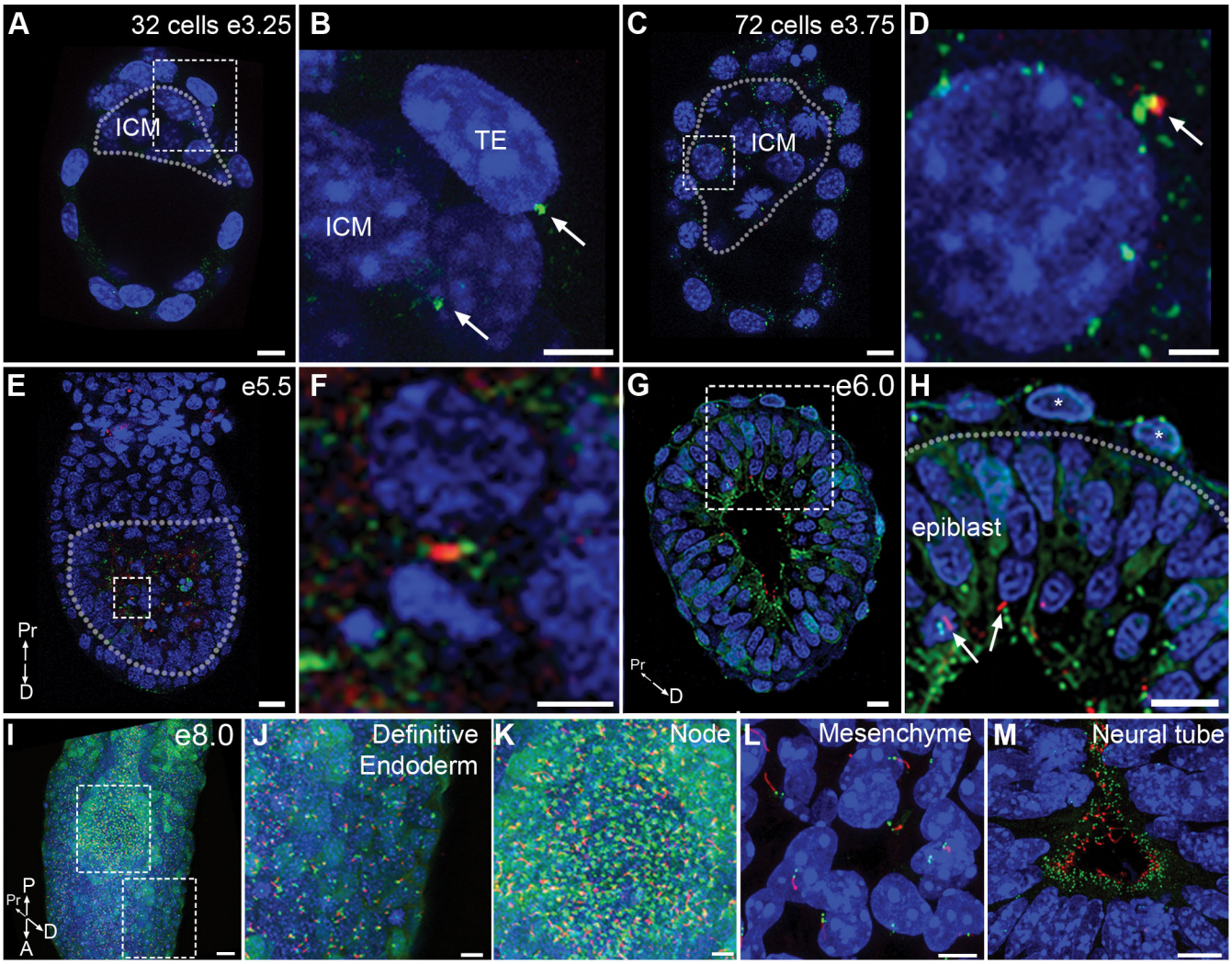

Figure 1. Primary cilia arise in the post-implantation epiblast

Embryos homozygous for the ARL13B-mCherry (red) and Centrin2-GFP (green) transgenes reveal the distribution of centrosomes and primary cilia in the early mouse embryo. (A–D) Preimplantation embryos. (A) Optical section of 32 cell early blastocyst (e3.25); dotted line surrounds ICM. (B) Expanded view of the dashed box in (A) shows that Centrin2-GFP positive centrioles are present on both trophectoderm cells (TE) and inner cell mass cells (ICM), arrows. No primary cilia are observed (Representative image selected from 4 embryos). (C) Optical section of a 72 cell blastocyst (e3.75); dotted line surrounds ICM. No cilia were detected on trophectoderm cells (0 cilia/255 cells from 9 embryos). (D) Expanded view of dashed box shown in (C) shows a rare example (2/107 cells scored from 9 embryos) of ARL13B-mCherry (arrow) expression adjacent to a Centrin2-GFP+ centriole of an ICM cell; these puncta did not have the morphology of cilia nor did they express acetylated α-tubulin. (E–H) Early postimplantation embryos. (E) Longitudinal optical section of e5.5 cavitating embryo; dotted line surrounds the epiblast. (F) Expanded view of the box in (E) shows a rare cilium on an epiblast cell (3/654 cells from 10 embryos). (G) Transverse optical section on an e6.0 embryo, with cilia exclusively on epiblast cells (388/1039 cells

from 6 embryos). (H) Expanded view of dashed box in (G) shows cilia (arrows) on epiblast cells; no cilia are present on Centrin2-GFP labeled centrioles in visceral endoderm cells (asterisks; 0/837 cells from 6 embryos). Dotted line denotes boundary between epiblast (below) and visceral endoderm (above). (I) Primary cilia are detected on nearly all cells of the e8.0 embryo. (J, K) Expanded views of dashed boxes in (I) show the cilia in the definitive endoderm (J) and node (K). (L, M) Sections of e10.5 embryos. Cilia are detected in nearly all cells in the limb mesenchyme (L). Neural progenitors extend cilia into the lumen of the neural tube (M). Nuclei are marked with DAPI (blue). Scale bars: (A, B): 10 μm; (C): 8 μm; (D): 2 μm (E): 20 μm; (F): 5 μm; (G, H): 20 μm; (I) 30 μm; (J, K): 10 μm; (L, M) 5 μm. P = posterior, A = anterior, Pr = proximal, D = distal.

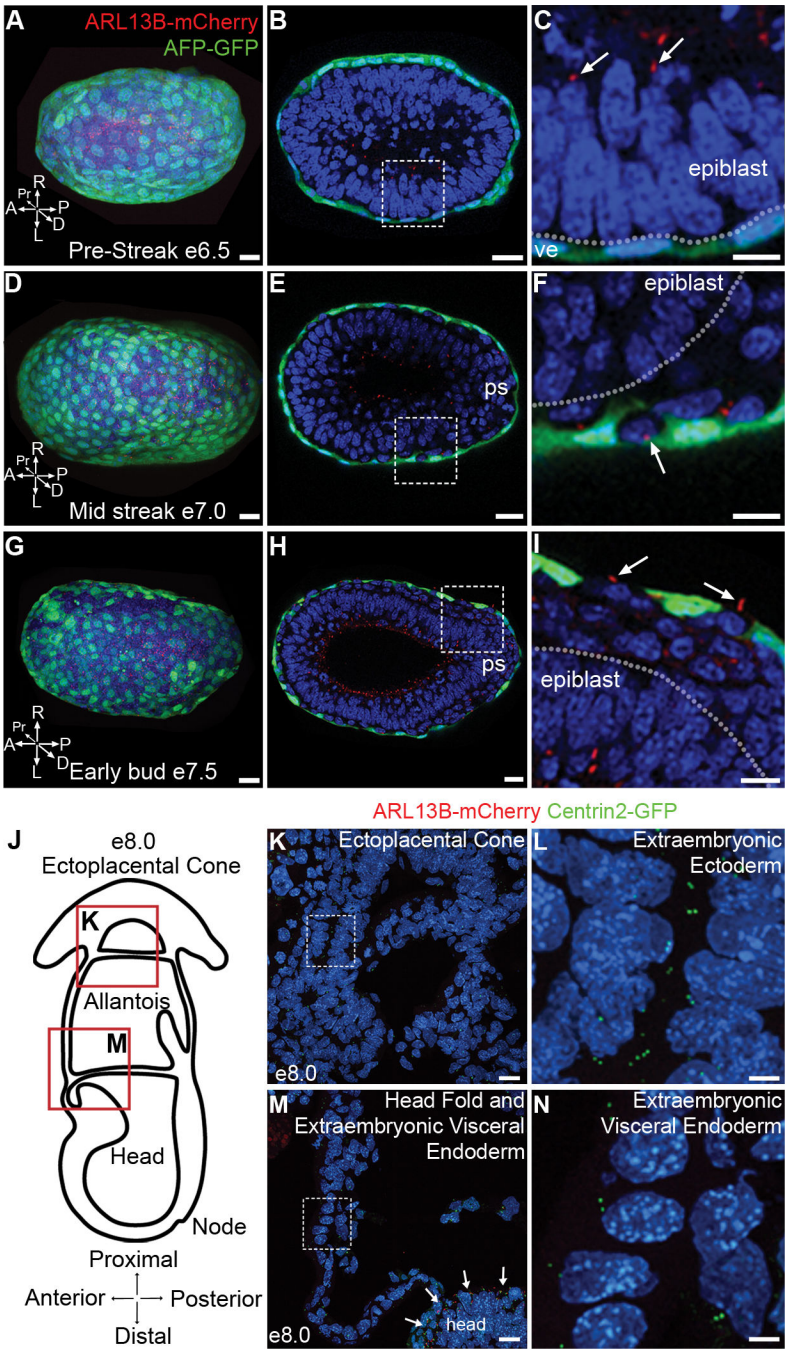

Figure 2. Primary cilia are restricted to embryonic lineages in late gastrulation stage embryos

(A–C) Primary cilia labeled with ARL13B-mCherry (red) are present on epiblast cells but are absent from cells of the visceral endoderm marked with AFP-GFP (green). (A) Distal view of pre-streak stage embryo (e6.5; Representative image selected from 4 embryos) expressing AFP-GFP and ARL13B-mCherry. (B) Transverse optical section of embryo in (A). (C) Magnification of dashed box in (B) shows presence of primary cilia labeled with ARL13B-mCherry (red) on epiblast cells, (arrow), but absent from visceral endoderm cells (ve), labeled with AFP-GFP (green). Dotted line denotes boundary between epiblast (above)

and visceral endoderm (below). (D–I) As the definitive endoderm intercalates with the visceral endoderm (green), cilia (red) are present on the definitive, but not the visceral, endoderm. (D) Distal view of mid-streak stage embryo (e7.0; Representative image selected from 3 embryos) expressing AFP-GFP and ARL13B-mCherry. (E) Transverse optical section of embryo in (D), primitive streak (ps) is to the right. (F) Magnification of dashed box in (E) shows that primary cilia are present on definitive endoderm cells, (arrow), but absent from surrounding visceral endoderm cells, labeled with AFP-GFP (green). Dotted line denotes boundary between epiblast and definitive endoderm. (G) Distal view of early bud stage embryo (e7.5) expressing AFP-GFP and ARL13B-mCherry (Representative image selected from 3 embryos). (H) Transverse optical section of embryo in (G), primitive streak (ps) is to the right. (I) Expanded view of box in (H) shows primary cilia on definitive endoderm cells (arrows) that have intercalated between AFP-GFP+ visceral endoderm cells (green). Dotted line denotes boundary between epiblast (below) and definitive endoderm (above). P = posterior, A = anterior, Pr = proximal, D = distal, L = left, R = right. (J) Schematic of e8.0 embryo in cross section illustrates the locations of images shown in (K) and (M). (K) Cells of the ectoplacental cone (derivatives of trophoblast lineage) expressing ARL13B-mCherry and Centrin2-GFP. (L) Magnification of dashed box in (K) shows Centrin2-GFP labeled centrioles with no primary cilium on extraembryonic ectoderm cells. (M) Cells of the extraembryonic visceral endoderm expressing ARL13B-mCherry and Centrin2-GFP are not ciliated, although epiblast cells in the headfolds are ciliated, arrows. (N) Magnification of dashed box (M) shows Centrin2-GFP labeled centrioles but no primary cilia on extraembryonic visceral endoderm cells. Nuclei are marked with DAPI (blue). Scale bars: (A–F) 30 μm; (G–I) 40 μm; (K, M) 20 μm; (L, N) 5 μm.

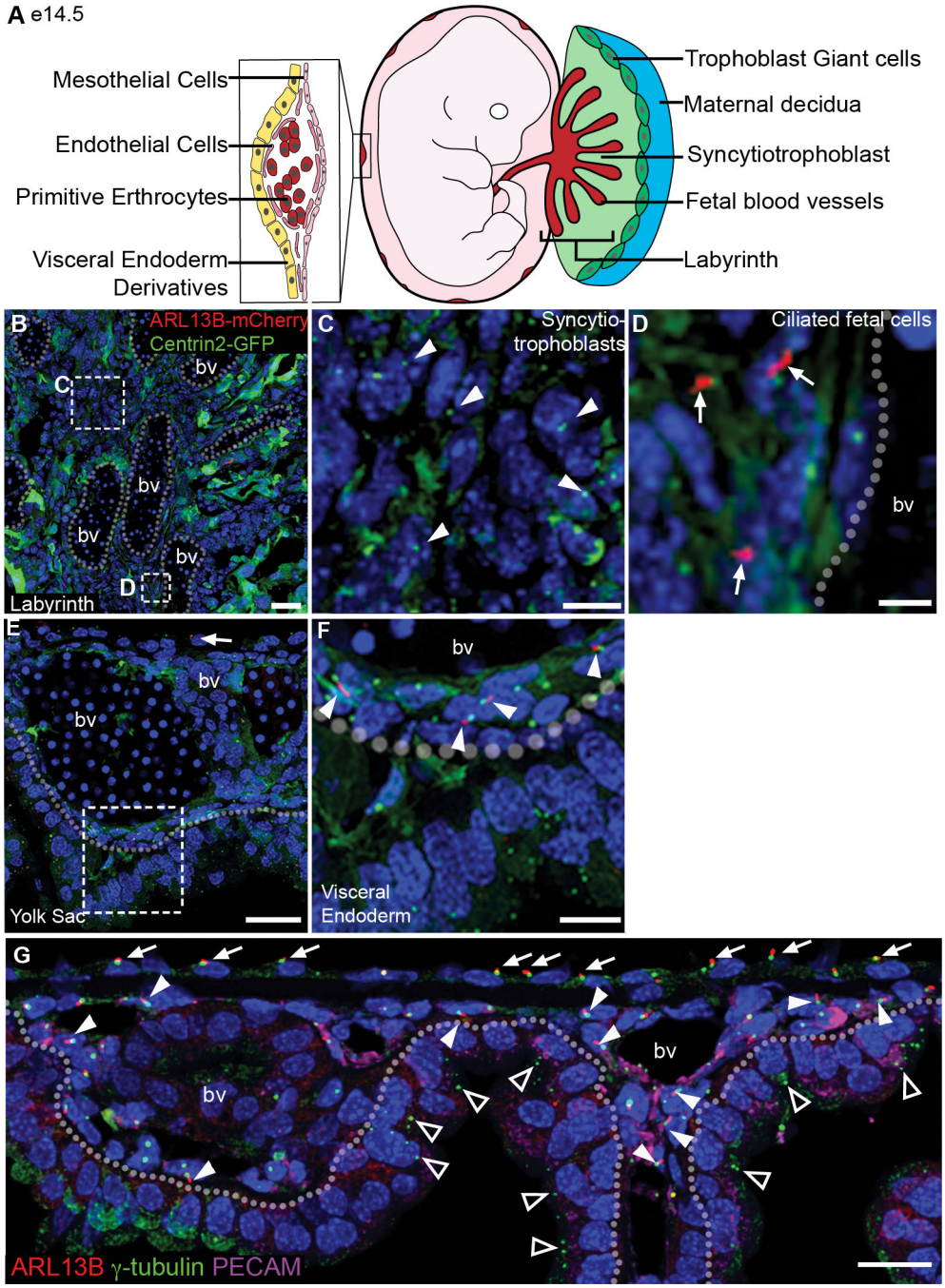

Figure 3. Extraembryonic lineages of the placenta and yolk sac lack cilia at e14.5

(A) Schematics of the placenta and yolk sac: trophoblast giant cells (dark green), spongiotrophoblast (light green), labyrinth (red), and magnified view of the yolk sac, illustrating a blood vessel surrounded by endothelial cells (dark pink) and the positions of mesothelial cells (light pink) and extraembryonic visceral endoderm derivatives (yellow). (B) Section of e14.5 labyrinth layer from an ARL13B-mCherry Centrin2-GFP placenta; dotted lines outline fetal blood vessels (bv). (C) Magnified view of box in (B), non-ciliated trophoblast-derived syncytiotrophoblast cells between fetal blood vessels lack cilia;

arrowheads indicate Centrin2-GFP+ centrioles. (D) Magnified view of box in (B), showing cilia on mesoderm derived cells surrounding fetal blood vessels (arrows). (E) Section of e14.5 yolk sac expressing ARL13B-mCherry and Centrin2-GFP; dashed line demarcates the boundary between mesoderm-derived cells (mesothelial and endothelial cells, above) and extraembryonic visceral endoderm-derived cells (below). Arrow indicates ciliated mesothelial cell. (F) Magnified view of box in (E) shows ciliated endothelial cells, (arrows) while extraembryonic visceral endoderm cells, below dashed line, are not ciliated. (F) Section of e14.5 yolk sac; dotted line demarcates the boundary between mesoderm-derived cells (mesothelial and endothelial cells, above) and extraembryonic visceral endoderm-derived cells (below). Antibody staining for γ-tubulin, labels centrosomes (green), and ARL13B, labels cilia (red), are present on mesothelial cells (arrows), and PECAM-expressing (magenta) endothelial cells (arrow heads). Extraembryonic visceral endoderm-derived cells have centrosomes (triangles) but no cilia (221/386 mesothelial cells; 95/292 endothelial cells; 0/1032 extraembryonic visceral endoderm-derived cells from 2 embryos). bv= blood vessel. Nuclei are marked with DAPI (blue). Scale bars: (B) 30 μm; (C,D) 10 μm; (E) 30 μm; (F) 10 μm; (G) 20 μm.

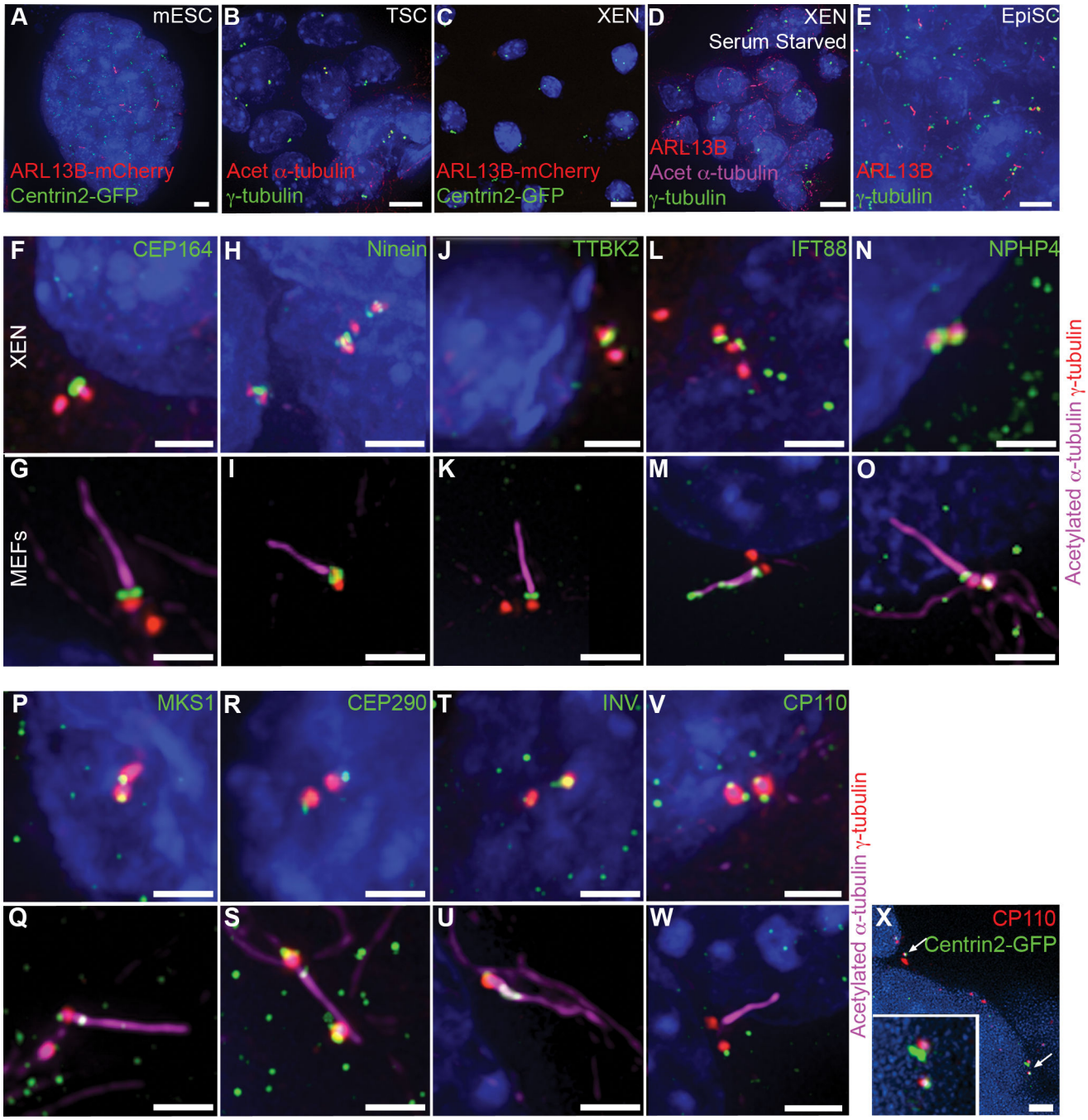

Figure 4. Embryo-derived stem cells recapitulate the cilia status of embryonic lineages

(A–E) Presence of primary cilia on embryo-derived stem cells. (A) 18% of asynchronously dividing mESCs derived from ARL13B-mCherry (red) Centrin2-GFP (green) transgenic embryos grown in 2i medium are ciliated. (B) Antibody staining for γ-tubulin (green) and acetylated α-tubulin (red) shows TS cells lack primary cilia. (C) No cilia are detected on XEN cells derived from ARL13B-mCherry Centrin2-GFP transgenic embryos. (D) Antibody staining for ARL13B (red) and acetylated α-tubulin (magenta) shows that serum starved XEN cells lack cilia (0/267 cells from 2 independent experiments). (E) Antibody

staining of EpiSCs for γ-tubulin (green) and ARL13B (red) shows that almost all EpiSCs are ciliated. (F–U) XEN cells have mature basal bodies. Centrioles marked with γ-tubulin (red) are associated with the distal appendage marker Cep164 (green) (F) and subdistal appendage marker ninein (green)(H). Positive regulators of ciliogenesis TTBK2 (green) (J) and IFT88 (green) (L) as well as transition zone proteins (green) NPHP4 (N), MKS1 (P), CEP290 (R) and Inversin (T) are also present at the mother centriole in XEN cells. (G, I, K, M, O, Q, S, U) Localization of basal body proteins in ciliated mouse embryonic fibroblasts (MEFs) is the same as in XEN cells, although IFT88 is also present in the axoneme in MEFs marked with acetylated α-tubulin (magenta). The negative regulator of ciliogenesis CP110 (green) is present on both centrioles in all XEN cells (V) but is removed from the mother centriole upon cilia assembly in MEFs (W). CP110 (red) is also present on both centrioles marked with Centrin2-GFP (green) in cells of the embryonic visceral endoderm (X, arrows). Nuclei are marked with DAPI (blue). Scale bars: (A–E) 7 μm; (F–W) 2 μm; (X) 3 μm.

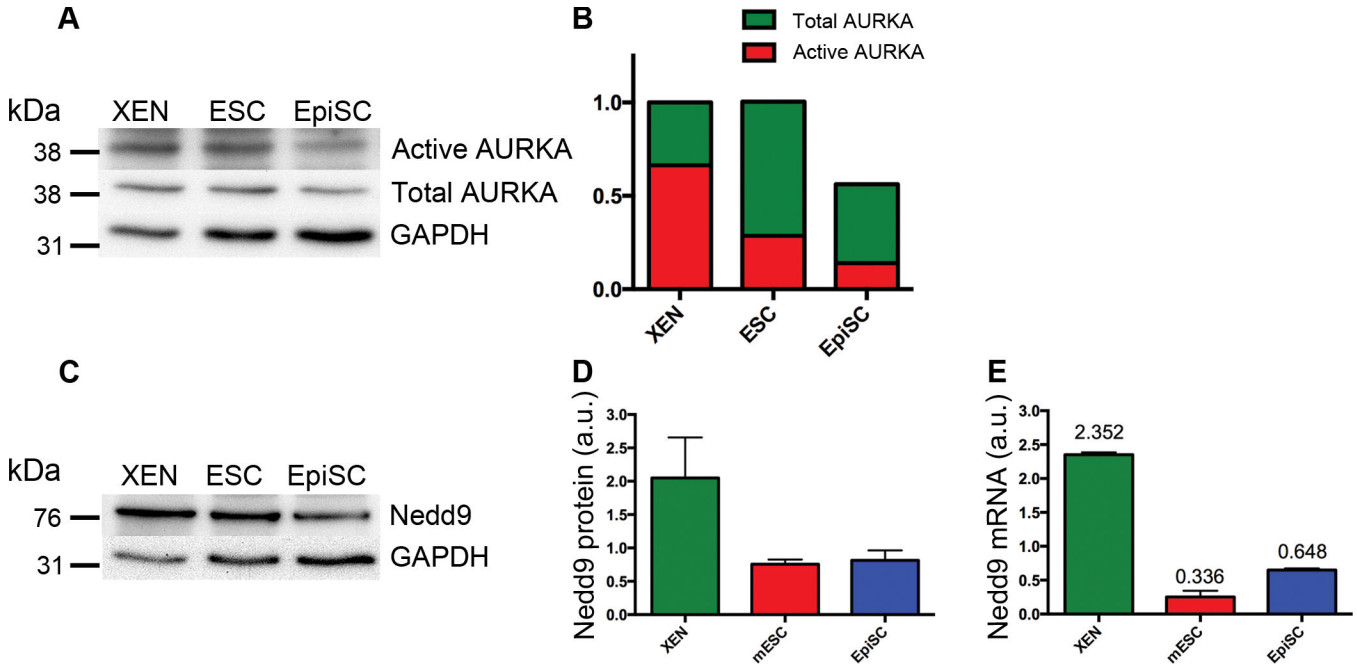

Figure 5. Components of the cilia disassembly pathway are highly expressed in XEN cells

(A) Western blot analysis of activated and total AURKA. (B) Quantification of the western blots for total AURKA (green) and activated AURKA (red), (n=3 independent experiments, normalized to XEN). (C) Western blot analysis of NEDD9 protein levels. (D) Quantification of Western blot analysis (C) shows that NEDD9 protein levels are 2.64 ± 1.15 fold higher in XEN cells compared to EpiSCs (n=3 independent experiments). Error bars indicate standard deviation. (E) *Nedd9* mRNA levels are higher in XEN cells than in EpiSCs by qPCR (values indicate mean mRNA expression levels, n=3 independent experiments). Error bars indicate standard deviation.

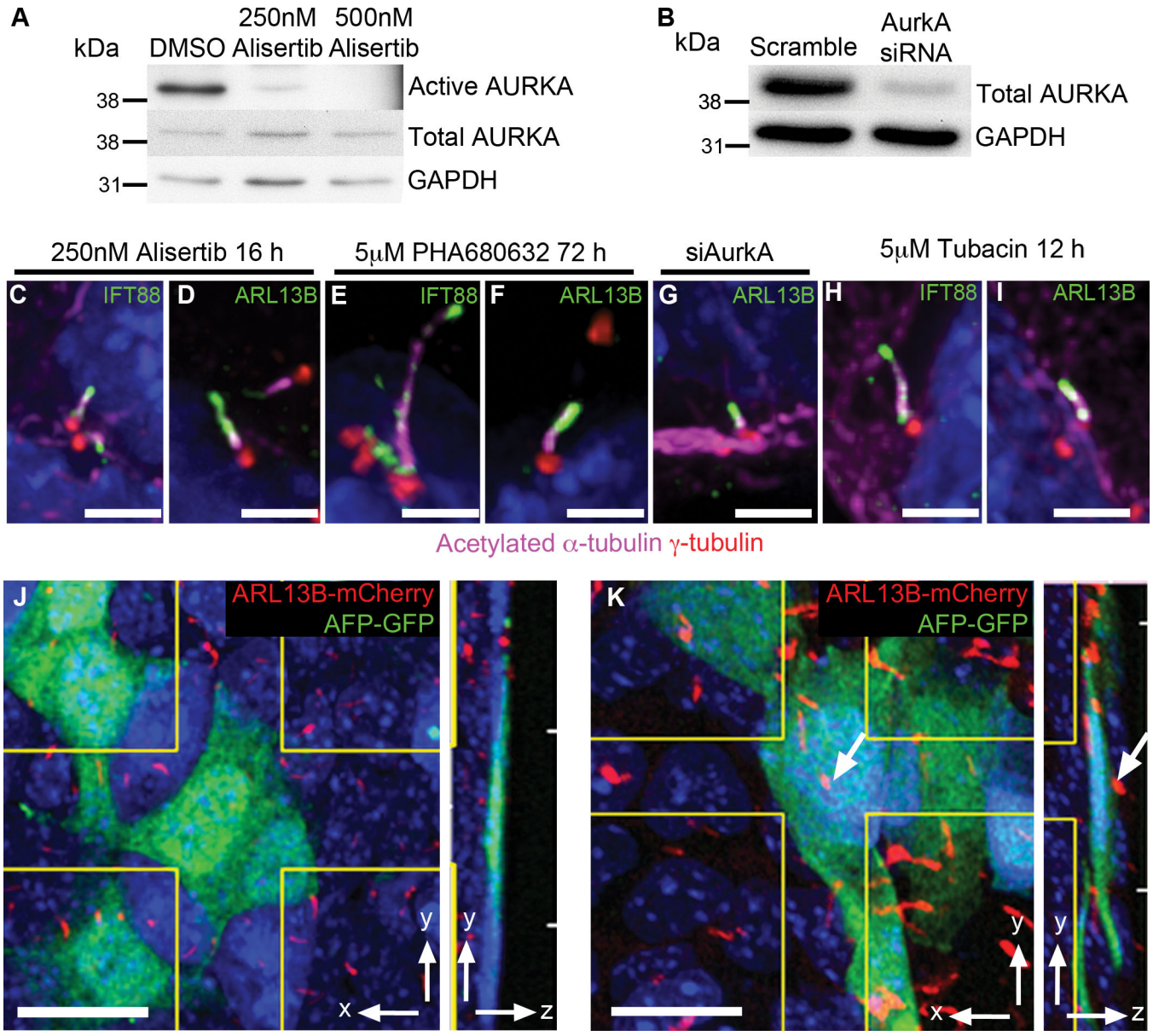

Figure 6. XEN and VE cells form cilia when the cilia disassembly pathway is inhibited

(A) Western blot shows that treatment for 16 h with 250 nM Alisertib reduces levels of phosphorylated AurkA by 32.5-fold compared to DMSO controls. Phosphorylated AurkA was not detected in cells treated with 500 nM Alisertib, whereas total AurkA levels are unaffected (n=2 independent experiments). (B) Western blot analysis shows that siRNA knock down of AurkA reduces levels of total AurkA to ~15 of control levels (n=2 independent experiments). (C, D) Treatment of XEN cells with 250 nM AURKA inhibitor Alisertib for 16h causes formation of primary cilia marked with IFT88 (C, green), ARL13B (D, green), and acetylated α-tubulin (magenta) labeled axoneme projecting from a centrosome marked with γ-tubulin (red; 20/328 cells). (E, F) Treatment of XEN cells with 5 μM AurkA inhibitor PHA680632 for 72 h causes formation of primary cilia marked with IFT88 (E, green), ARL13B (F, green) and acetylated tubulin (magenta) projecting from a

centrosome marked with γ-tubulin (red; 15/302 cells). (G) siRNA knock down of AurkA causes formation of primary cilia on XEN cells marked with ARL13B (green) and acetylated α-tubulin (magenta) projecting from a centrosome marked with γ-tubulin (red; 7/610 cells from 2 independent experiments). (H, I) Treatment of XEN cells with 5 μM HDAC6 inhibitor tubacin for 12 h causes formation of primary cilia on XEN cells marked with IFT88 (H), ARL13B (I) and acetylated α-tubulin (magenta), projecting from a centrosome marked with γ-tubulin (red; 8/717 cells from 3 independent experiments). (J, K) Culture of e7.5 embryos for 12h in 5 μM tubacin causes cilia formation (red) on visceral endoderm cells (green). (J) Visceral endoderm cells in an e7.5 embryo expressing AFP-GFP (green) are never ciliated in DMSO treated control embryos (0/1263 cells counted across 6 embryos). (K) Primary cilia, labeled with ARL13B-mCherry (red) are observed on AFP-GFP (green) visceral endoderm cells in embryos cultured with 5 μM tubacin for 12 h (30/1313 cells counted across 7 embryos). Arrow indicates a primary cilium present on this AFP-GFP+ cell. Side panels show yz view. Nuclei stained with DAPI (blue). Scale bars = (C–I) 2 μm; (J, K) 20 μm.